



A microscopic and nanoscopic view of storm-time choruson 31 March 2001

O. Santolik, D.A. Gurnett, J.S. Pickett, Michel Parrot, N. Cornilleau-Wehrlin

► To cite this version:

O. Santolik, D.A. Gurnett, J.S. Pickett, Michel Parrot, N. Cornilleau-Wehrlin. A microscopic and nanoscopic view of storm-time choruson 31 March 2001. *Geophysical Research Letters*, 2004, 31 (2), pp.L02801. 10.1029/2003GL018757 . hal-00153125

HAL Id: hal-00153125

<https://hal.science/hal-00153125>

Submitted on 25 Jan 2016

HAL is a multi-disciplinary open access archive for the deposit and dissemination of scientific research documents, whether they are published or not. The documents may come from teaching and research institutions in France or abroad, or from public or private research centers.

L'archive ouverte pluridisciplinaire **HAL**, est destinée au dépôt et à la diffusion de documents scientifiques de niveau recherche, publiés ou non, émanant des établissements d'enseignement et de recherche français ou étrangers, des laboratoires publics ou privés.

A microscopic and nanoscopic view of storm-time chorus on 31 March 2001

O. Santolík,¹ D. A. Gurnett, and J. S. Pickett

Department of Physics and Astronomy, University of Iowa, Iowa City, USA

M. Parrot

LPCE/CNRS, Orléans, France

N. Cornilleau-Wehrlin

CETP/IPSL, Vélizy, France

Received 2 October 2003; revised 31 October 2003; accepted 19 November 2003; published 21 January 2004.

[1] We investigate intense whistler-mode chorus emissions which occurred during the geomagnetic storm on 31 March 2001. We use multipoint measurements obtained by the Cluster spacecraft in the premidnight equatorial region outside the plasmasphere at a radial distance of 4 Earth radii ($L = 4.0 - 4.2$). Observed spatio-temporal variations of the direction of the Poynting flux manifest a consistent pattern: the central position of the chorus source fluctuates at time scales of minutes within 1000–2000 km of the geomagnetic equator. We demonstrate that estimates of the electromagnetic planarity can be used to characterize the extent of the source, obtaining a range of 3000–5000 km. Discrete wave packets of chorus are observed to rise in frequency between 0.13 and 0.5 of the local electron cyclotron frequency, at a rate up to 20 kHz/s, having the maximum peak amplitudes of ~ 20 mV/m. We observe a fine structure of subpackets with large amplitudes embedded in the interior of the wave packets. This fine structure has a typical delay of a few milliseconds between the two neighboring maxima of the wave amplitude. Longer delays occur with a decreasing probability density.

INDEX TERMS: 2730 Magnetospheric Physics: Magnetosphere—inner; 2772 Magnetospheric Physics: Plasma waves and instabilities; 2778 Magnetospheric Physics: Ring current; 6984 Radio Science: Waves in plasma. **Citation:** Santolík, O., D. A. Gurnett, J. S. Pickett, M. Parrot, and N. Cornilleau-Wehrlin (2004), A microscopic and nanoscopic view of storm-time chorus on 31 March 2001, *Geophys. Res. Lett.*, 31, L02801, doi:10.1029/2003GL018757.

1. Introduction

[2] On March 31, 2001, a major interplanetary disturbance compressed the Earth's magnetosphere, pushing the magnetopause and bow shock inside of the geosynchronous orbit [Ober *et al.*, 2002]. The event was accompanied by a strong southward interplanetary magnetic field and produced a significant geomagnetic activity, strongly perturbing the geomagnetic field (K_p index was 9[−] between 0300 and 0900 UT). The storm time was reflected by the hourly

equatorial Dst index dropping from +30 nT at 0400 UT down to −358 nT at 0900 UT. Skoug *et al.* [2003] concluded that the storm main phase was dominated by tail currents flowing close to the Earth until the dipolarization of the magnetic field occurred at ~ 0630 UT. Baker *et al.* [2002] reported observations of dispersionless injection of energetic electrons in the pre-midnight sector, accompanied by a strong magnetospheric substorm with the AE index reaching ~ 1200 nT. They presented a microscopic view of this substorm obtained by the Cluster spacefleet. The four Cluster spacecraft crossed the substorm injection boundary between 0634 and 0640 UT at the geocentric radial distance of 4.2 Earth radii (R_E) and approximately $1.4 R_E$ to the South of the geomagnetic dipole equator. The spacefleet then continued to move northward and observed increasing fluxes of electrons at energies of 39–51 keV [see Figure 1a of Baker *et al.*, 2002] until shortly after 0700 UT when the fluxes reached a maximum and started to diminish. Between 0706 and 0713 UT, close to their perigee, the four Cluster spacecraft successively passed through the geomagnetic equatorial plane at a radial distance of $\sim 4 R_E$ and at ~ 2200 MLT.

[3] It has been previously shown [e.g., Tsurutani and Smith, 1974; Anderson and Maeda, 1977] that the injection of substorm electrons leads to the excitation of intense whistler-mode chorus emissions in the vicinity of the geomagnetic equator outside of the plasmasphere. These waves, in turn, can accelerate the electrons in the Earth's outer radiation belt to relativistic energies [Meredith *et al.*, 2003] causing radiation damage to Earth orbiting spacecraft. The source mechanism of the intense wave packets of chorus is not yet fully understood. It is generally believed that chorus is generated by a nonlinear process [e.g., Nunn *et al.*, 1997; Trakhtengerts, 1999] based on the electron cyclotron resonance of electromagnetic whistler-mode waves with energetic electrons. On 31 March 2001, when the Cluster spacefleet arrived at the equatorial region at $L = 4.0 - 4.2$, it was surrounded by a low density plasma of a few particles per cc, staying thus well outside the plasmasphere (P. Décréau, private communication, 2002), and observing large fluxes of energetic electrons [Baker *et al.*, 2002]. The conditions were thus very favorable for the excitation of chorus. Indeed, the wave spectrum analyzers onboard Cluster observed strong chorus emissions propagating from a source region located within 3° of the geomagnetic equator [Parrot *et al.*, 2003].

¹Now at Faculty of Mathematics and Physics, Charles University, Prague, and at Institute of Atmospheric Physics, Czech Academy of Sciences, Prague, Czech Republic.

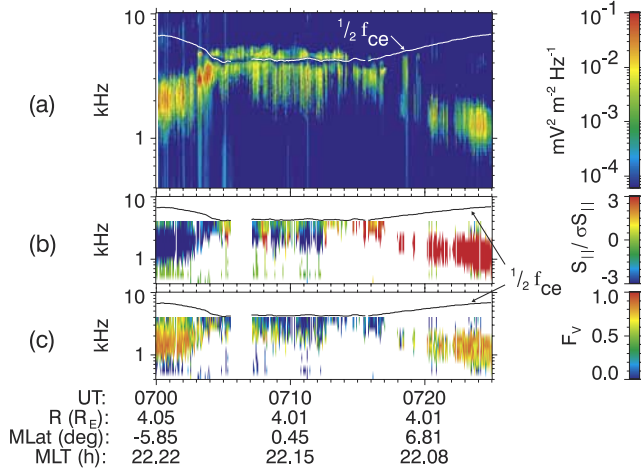


Figure 1. (a) Time-frequency power spectrogram of electric field fluctuations recorded on board Cluster 3 on March 31, 2001. (b) Parallel component of the Poynting vector normalized by its standard deviation. (c) Electromagnetic planarity. Position is given on the bottom: R-radial distance; MLat-magnetic dipole latitude; MLT-magnetic local time.

[4] The aim of the present letter is to report our detailed analysis of the dynamics of this source region. First, we analyze time scales of several minutes, similar to the “microscopic” view of the substorm injection boundary presented by *Baker et al.* [2002]. Then, we present a “nanoscopic” view descending down to the time intervals of tens of microseconds, i.e., 10^{-9} of the typical substorm time scale. We use observations of the Cluster spacecraft recorded between 0700 and 0725 UT on 31 March 2001, when the spacecraft crossed the source region of chorus. Our analysis is based on high-resolution measurements of the wideband (WBD) wave instruments [*Gurnett et al.*, 2001], and on the multi-dimensional data of the spectrum analyzers of the STAFF instruments [*Cornilleau-Wehrin et al.*, 2003].

2. Multipoint Measurement of the Chorus Source

[5] During the perigee pass on 31 March 2001, the WBD instruments were set up to continuously record waveforms using a pass-band filter between 80 Hz and 19 kHz, with a sampling frequency of 55 kHz. Electric double-sphere antennas (88 m long) were used as sensors. Of the four spacecraft, WBD data from two (Cluster 1 and Cluster 3) are available. Figure 1a shows an overview time-frequency power spectrogram calculated from the data recorded by WBD on board Cluster 3. The spacecraft moved along its orbit through the equatorial region from the South to the North. The geomagnetic disturbances were reflected by variations of the ambient magnetic field: the white line in Figure 1a shows one half of the local electron cyclotron frequency ($\frac{1}{2}f_{ce}$). The intense chorus emissions are organized into two frequency bands [*Anderson and Maeda*, 1977]. The upper band appears only in the region of depressed magnetic field around the geomagnetic equator and its lower-frequency limit follows the local $\frac{1}{2}f_{ce}$. The lower band of chorus below $\frac{1}{2}f_{ce}$ continues in both hemi-

spheres towards higher magnetic latitudes, decreasing in frequency.

[6] This lower band consists of right-hand polarized (whistler-mode) electromagnetic waves as determined from simultaneous measurements of the STAFF-SA instruments (not shown). These instruments perform multidimensional spectral analysis using three magnetic and two electric components with a time resolution of 4 s, a frequency resolution of 25%, and with an upper frequency limit of 4 kHz. From relative phase shifts of the electric and magnetic field fluctuations we estimate the parameter $S_{||}/\sigma S_{||}$ proportional to the projection $S_{||}$ of the Poynting vector onto the direction of the ambient magnetic field (\mathbf{B}_0). The normalization factor $\sigma S_{||}$ corresponds to the standard deviation of $S_{||}$ induced by the spectral analysis. Results in Figure 1b show that the Poynting flux has a significant southward component (blue) at magnetic latitudes below -3.5° , and a northward component (red) at magnetic latitudes above 3.5° . Taking into account propagation properties of the whistler-mode waves, it means that the Poynting flux diverges. This indicates that the source region of the lower band of chorus is localized close to the equatorial plane, as found previously by *LeDocq et al.* [1998]. The STAFF-SA data, measured simultaneously on the other three Cluster spacecraft, give results leading to the same conclusion, as documented by *Parrot et al.* [2003]. An independent estimate of the source position is given in Figure 1c showing the electromagnetic planarity estimator F_V [equation 37 of *Santolík et al.*, 2003a]. Its value is between 0 (blue) and 1 (red), 1 corresponding to the presence of waves well characterized by a single wave vector. F_V tends to 0 when a mixture of waves propagating in antiparallel directions is observed. Our results show that, at higher latitudes, F_V approaches unity as the waves propagate from their source. F_V is close to zero at latitudes between -4° and $+5.5^\circ$, indicating that chorus propagates here in both directions at the same time. This is exactly what we would expect to find inside a source region emitting the waves to both hemispheres. Outside the source, typical angles between the wave vector and \mathbf{B}_0 increase from values below 15° up to $\sim 50^\circ$ (not shown), indicating unducted propagation.

[7] Combining now the measurements of the four Cluster spacecraft, as recorded along their respective orbits, we can verify if there is a consistent spatio-temporal pattern of wave propagation properties. Figure 2 shows that it is always possible to find a distance from the geomagnetic equator where the integral Poynting flux (500 Hz–4 kHz) changes its sign. The simultaneous observations of the four spacecraft can thus be coherently explained by motion of this central source position along the Z_{SM} axis (perpendicular to the geomagnetic equator). The resulting position $Z_{SM}^*(t)$ is shown by the purple line in Figure 2. It is, at each time t , calculated by linear interpolation of $S_{||}/\sigma S_{||}$ between the positions of the two spacecraft where the Poynting flux changes its sign. If this sign is the same at all the spacecraft, $Z_{SM}^*(t)$ is estimated from the position $Z_{SM}^m(t)$ of the spacecraft where $S_{||}/\sigma S_{||}$ is minimum,

$$Z_{SM}^*(t) = Z_{SM}^m(t) - \alpha(S_{||}/\sigma S_{||})_{\min},$$

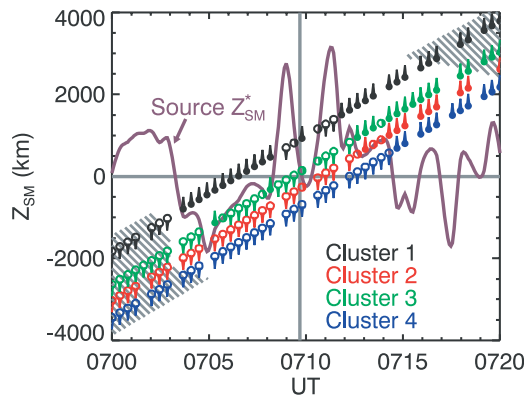


Figure 2. Z_{SM} coordinate of the four color-coded Cluster spacecraft as a function of time. Sign of the parallel component of the Poynting flux is shown by downward arrows attached to the open symbols, and by upward arrows with the solid symbols, for southward and northward components, respectively. The half-filled symbols with no arrows indicate that the sign cannot be reliably determined. Horizontal grey line is at the magnetic equator, vertical grey line shows the time when center of mass of the four spacecraft crosses the equatorial plane. Shaded areas bound the regions of low F_V values. Purple line shows the calculated position where the Poynting flux changes its sign.

where $\alpha \approx 430$ km is calculated from a linear fit to the obtained $S_{||}/\sigma S_{||}$ values as a function of Z_{SM} .

[8] Figure 2 shows that the resulting central source position flaps within 1000–2000 km of the geomagnetic equator on time scales of minutes. This obtained extent does not necessarily reflect the dimension of the source measured perpendicular to the equator. It only shows the dynamics of a source's central position defined by the integral Poynting flux. On the other hand, the dimension of the source, at least with respect to the wave propagation, is reflected by the electromagnetic planarity F_V . The shaded areas in Figure 2 show the approximate boundaries of the low- F_V intervals for the four spacecraft. These intervals are ~ 3000 – 5000 km long in the direction perpendicular to the geomagnetic equator, as traced by the spacecraft along their orbit. The obtained range roughly corresponds to theoretical estimates of the dimension of the source region of chorus [e.g., *Trakhtengerts*, 1999].

3. Analysis of Chorus Wave Packets

[9] Figure 2 shows that there are intervals of time where Cluster 1 and Cluster 3 observe opposite directions of the integral Poynting flux. These intervals could be a good opportunity to verify if the source emits the same chorus wave packets symmetrically to the South and to the North. We have thus analyzed detailed spectrograms calculated from the WBD data during the entire passage through the source region. The observed discrete elements of chorus rise in frequency from as low as 1 kHz up to ~ 4 kHz (0.13 – $0.5 f_{ce}$) at an overall rate of 10–20 kHz/s. Sometimes, much less structured hiss-like emissions, or their combination with discrete elements are observed.

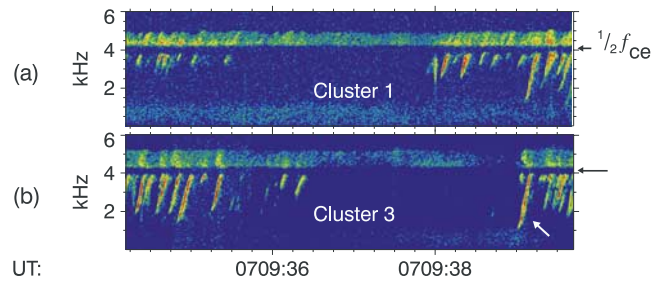


Figure 3. Detailed time-frequency power spectrograms of electric field fluctuations in the source region recorded on board (a) Cluster 1, and (b) Cluster 3, respectively. The color scale in $\text{mV}^2 \text{m}^{-2} \text{Hz}^{-1}$ is the same as in Figure 1a. Black arrows on the right indicate local $\frac{1}{2}f_{ce}$ for each spacecraft.

[10] Figure 3 shows an example of detailed spectrograms of electric field fluctuations from Cluster 1 and 3. Both spacecraft are in the region of low F_V and the central position of the source derived from the Poynting flux is between them. We can identify the two chorus bands, the lower band showing discrete elements. The element marked by a white arrow in Figure 3b rises between 1 and 4 kHz at a rate of 19 kHz/s. At the first sight, it seems to have a counterpart in Figure 3a, but a detailed analysis shows that their timing delay is much longer than the maximum expected group delay of whistler-mode waves. Similarly, we have found no evidence of correlation of the discrete elements recorded on the two spacecraft throughout the source region. This still does not rule out the possibility of a symmetric radiation, since the two spacecraft are at relatively large separations of ~ 800 km along B_0 , and ~ 300 km perpendicular to B_0 . Notably, the separation perpendicular to B_0 is larger than the characteristic correlation length of chorus elements found for another storm-time case on 18 April 2002 *Santolik and Gurnett* [2003].

[11] *Santolik et al.* [2003b] showed for the same case of 18 April 2002 that the chorus wave packets are composed of a system of subpackets, changing their amplitudes on time

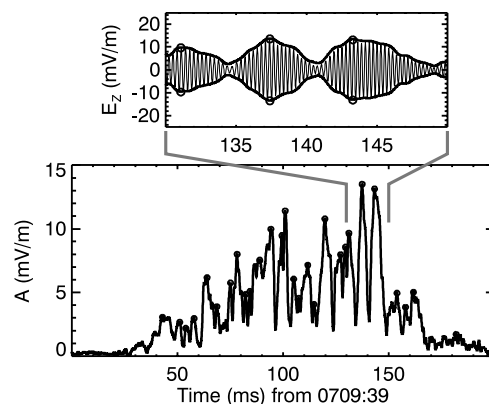


Figure 4. Example of the fine structure of amplitudes of the electric field fluctuations as a function of time. The corresponding chorus element is shown by the white arrow on Figure 3b. Local maxima are marked by open circles. The inset on the top shows a short fraction of the signal, its envelope, and local maxima.

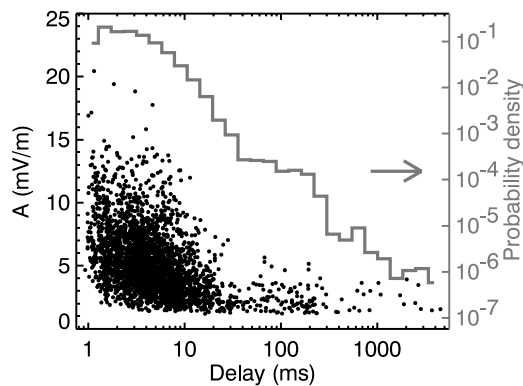


Figure 5. Scatter plot of local maxima of the amplitudes of the electric field fluctuations versus the time delays between them. Histogram of time delays between the local maxima is plotted by the gray line with the right-hand side vertical scale.

scales of a few milliseconds. We may thus expect a similar fine structure embedded in the chorus wave packets observed on 31 March 2001. Indeed, Figure 4 shows such a fine structure for the example time interval from Figure 3b. We use here an analysis method different from that used by Santolík *et al.* [2003b], looking only at broadband amplitudes of the signal. The signal is first convolved with a pass-band non-recursive filter between 2 and 4 kHz, and then, the maxima of its absolute values are found in consecutive 0.5-ms subintervals. We thus obtain an estimate of the envelope of the signal with 0.5-ms time resolution, which is then interpolated back to the original sampling resolution (0.0182 ms) using cubic splines. The inset on the top of Figure 4 shows the resulting amplitude-envelope together with the signal. The analysis of the whole 200-ms interval shows that the chorus wave packet contains a complex structure of tens of subpackets with different amplitudes. According to the cold plasma theory, the maximum amplitude of 14 mV/m corresponds to ~ 150 pT in the magnetic component.

[12] Similar analysis has been done with all the Cluster 3 data in the time interval between 0709:15 and 0710:15 when the central positions of the source were close to the spacecraft. We have found 2911 local maxima with values up to 22.9 mV/m, separated by time intervals between 0.9 ms and 4.5 s. Figure 5 shows the results of this systematic analysis. Each solid black point corresponds to an average value of two neighboring local maxima plotted against the duration of the corresponding time interval between them. The gray line with the right-hand vertical scale shows the histogram of the probability density of obtained points in 28 logarithmic subintervals of delays between the maxima. We can see that most of the delays are of the order of a few ms, with the probability density decreasing towards longer delays until ~ 40 ms. Then, the probability density shows signs of a plateau, connected probably to the dominant delay of ~ 0.1 – 0.2 s between the chorus elements as seen on Figure 3. For longer delays the probability density steeply descends below the limits of statistical reliability. The scatter plot shows that the highest amplitudes are seen at short delays, corresponding to the

concentration of the large-amplitude subpackets in the interior of the chorus packets.

[13] A more detailed statistical analysis including larger intervals of data will be the subject of future work. More investigation is also needed to establish the primary cause of the observed fine structure. It may be inherent to the particular mode of wave generation, as is suggested by exponential growth or decay which are often connected with the subpackets of longer duration (>10 ms). The fine structure can also arise as a consequence of a simple superposition of narrowband signals at close frequencies. In this case the variation of the envelope would be close to sinusoidal, which also often corresponds to the observations.

4. Summary

[14] A multiscale analysis of the wave measurements collected by the Cluster spacefleet inside the source region of whistler mode chorus during the geomagnetic storm on 31 March 2001 leads us to the following new results:

[15] 1. Estimates of the electromagnetic planarity F_V give a dimension of the source parallel to B_0 in the range 3000–5000 km, consistent with theoretical predictions.

[16] 2. The central position of the source, defined with respect to the Poynting flux direction, flaps at time scales of minutes within 1000–2000 km of the geomagnetic equator.

[17] 3. A fine structure of subpackets inside the discrete wave packets of chorus has a typical delay of a few ms between the two neighboring maxima of the wave amplitude, with a decreasing probability density toward longer delays.

[18] 4. Large amplitude (up to ~ 20 mV/m) subpackets are found to be embedded in the interior of the chorus wave packets.

[19] **Acknowledgments.** We acknowledge discussions of the STAFF data with C. Harvey, M. Maksimovic, and Y. de Conchy. We thank P. Décréau and P. Canu for estimating the plasma density from the data of the Whisper experiment. We acknowledge discussions with I. H. Cairns, V. Y. Trakhtengerts, B. V. Kozelov, and A. G. Demekhov, and the access to the spin-resolution data of the FGM magnetic field experiment (PI A. Balogh) used for reference. This research was supported by the NASA Goddard Space Flight Center under Grant No. NAG5-9974. O. Santolík acknowledges additional support from grants MSM 113200004, ME 650, GACR 202/03/0832.

References

- Anderson, R. R., and K. Maeda (1977), VLF emissions associated with enhanced magnetospheric electrons, *J. Geophys. Res.*, **82**, 135.
- Baker, D. N., et al. (2002), A telescopic and microscopic view of a magnetospheric substorm on 31 March 2001, *Geophys. Res. Lett.*, **29**(18), 1862, doi:10.1029/2001GL014491.
- Cornilleau-Wehrin, N., et al. (2003), First results obtained by the Cluster STAFF experiment, *Ann. Geophys.*, **21**, 437–456.
- Gurnett, D. A., et al. (2001), First results from the Cluster wideband plasma wave investigation, *Ann. Geophys.*, **19**, 1259–1272.
- LeDocq, M. J., D. A. Gurnett, and G. B. Hospodarsky (1998), Chorus source locations from VLF Poynting flux measurements with the Polar spacecraft, *Geophys. Res. Lett.*, **25**(21), 4063–4066.
- Meredith, N. P., M. Cain, R. B. Horne, R. M. Thorne, D. Summers, and R. R. Anderson (2003), Evidence for chorus-driven electron acceleration to relativistic energies from a survey of geomagnetically disturbed periods, *J. Geophys. Res.*, **108**(A6), 1248, doi:10.1029/2002JA009764.
- Nunn, D., Y. Omura, H. Matsumoto, I. Nagano, and S. Yagitani (1997), The numerical simulation of VLF chorus and discrete emissions observed on the Geotail satellite using a Vlasov code, *J. Geophys. Res.*, **102**(A12), 27,083–27,097.

- Ober, D. M., M. F. Thomsen, and N. C. Maynard (2002), Observations of bow shock and magnetopause crossings from geosynchronous orbit on 31 March 2001, *J. Geophys. Res.*, *107*(A8), doi:10.1029/2001JA000284.
- Parrot, M., O. Santolík, N. Cornilleau-Wehrin, M. Maksimovic, and C. Harvey (2003), Source location of chorus emissions observed by CLUSTER, *Ann. Geophys.*, *21*(2), 473–480.
- Santolík, O., and D. A. Gurnett (2003), Transverse dimensions of chorus in the source region, *Geophys. Res. Lett.*, *30*(2), 1031, doi:10.1029/2002GL016178.
- Santolík, O., M. Parrot, and F. Lefeuvre (2003a), Singular value decomposition methods for wave propagation analysis, *Radio. Sci.*, *38*(1), 1010, doi:10.1029/2000RS002523.
- Santolík, O., D. A. Gurnett, J. S. Pickett, M. Parrot, and N. Cornilleau-Wehrin (2003b), Spatio-temporal structure of storm-time chorus, *J. Geophys. Res.*, *108*(A7), 1278, doi:10.1029/2002JA009791.
- Skoug, R. M., et al. (2003), Tail-dominated storm main phase: 31 March 2001, *J. Geophys. Res.*, *108*(A6), 1259, doi:10.1029/2002JA009705.
- Trakhtengerts, V. Y. (1999), A generation mechanism for chorus emission, *Ann. Geophys.*, *17*, 95–100.
- Tsurutani, B. T., and E. J. Smith (1974), Postmidnight chorus: A substorm phenomenon, *J. Geophys. Res.*, *79*, 118–127.
-
- O. Santolík, Faculty of Mathematics and Physics, Charles University, V Holešovičkách 2, CZ-18000 Praha 8, Czech Republic. (ondrej.santolik@mff.cuni.cz)
- D. A. Gurnett and J. S. Pickett, Department of Physics and Astronomy, University of Iowa, Iowa City, IA 52242-1479, USA. (gurnett@space.physics.uiowa.edu; jsp@space.physics.uiowa.edu)
- M. Parrot, LPCE/CNRS, 3A Avenue de la Recherche, Orléans, F-45071 France. (mparrot@cnrs-orleans.fr)
- N. Cornilleau-Wehrin, CETP/IPSL, 10/12 Avenue de L'Europe, F-78140 Velizy, France. (nicole.cornilleau@cetp.ipsl.fr)